Fast covariance propagation for two-line element sets

Blair F. Thompson, Jesse R. Gossner, Brandon J. Sais, Capt Elizabeth A. Cunningham
319th Combat Training Squadron, U.S. Air Force, Peterson Air Force Base, Colorado

ABSTRACT

We present a method for quickly propagating the covariance associated with a two-line element set (TLE). Based on general perturbation theory, TLEs are reasonably accurate and propagate the orbital state of a resident space object (RSO) relatively quickly over long periods of time, making them useful for certain first-order space situational awareness (SSA) analyses. However, TLEs are generally not published with covariance or other measures of uncertainty, making it difficult to model and determine uncertainty of the analyses results. In cases where the TLE covariance is available or can be estimated by some indirect method, the traditional method of propagating the covariance is numerical integration of the state transition matrix (STM) which involves integration of forty-two equations of motion, six equations for the orbital state (position and velocity) and thirty-six equations for the six-by-six state transition matrix. The numerical integration time significantly limits the usefulness for SSA purposes, especially when longer time spans or multiple space objects are involved. As a result, this type of processing loses much of the advantage of general perturbations techniques, namely generally faster state propagation. Because Lambert targeting is the solution of the fundamental boundary value problem of astrodynamics, a Lambert targeting routine can be used to estimate the effects of small position and velocity errors at some reference time on the errors at some future time, which is the essence of the state transition matrix. The method presented in this paper quickly propagates covariance by computing the STM using a Lambert targeting routine in lieu of numerical integration, enabling fast multi-rev (even multi-day) analyses commensurate with TLE accuracy. Furthermore, the fast method enables the estimation of state covariance of space objects from historical TLE data.

1. INTRODUCTION

Two-line elements (TLEs, or "elsets") are a specific type of mean orbital elements for modeling Earth orbiting objects. TLE's have been in use for decades, and will continue to be used into the foreseeable future, perhaps with some modification. The U.S. Air Force 18th Space Control Squadron uses TLEs as the basis for the public catalog of resident space objects (RSO) on the website space-track.org. The software required to make use of TLEs is also widely available in a variety of programming languages. However, TLEs are not published with covariance or other measures of uncertainty. When a TLE is pulled from a catalog, for example, there is no indication of how accurate the TLE is, how many and what type(s) of observations were used to create the TLE, the time span to which the TLE was fit, etc.

Based on general perturbation theory, TLEs are reasonably accurate and propagate the orbital state of a resident space object relatively quickly over long periods of time, making them useful for certain first-order space situational awareness (SSA) analyses. Because TLEs are generally not published with covariance or other measures of uncertainty, it is difficult to model and determine the uncertainty of the analyses results. In cases where the TLE covariance is available or can be estimated by some indirect method, the traditional method of propagating the covariance is numerical integration of the state transition matrix (STM) which involves integration of forty-two equations of motion – six equations for the orbital state (position and velocity) and thirty-six equations for the state transition matrix. The required numerical integration time significantly limits the usefulness for SSA purposes, especially when longer time spans or multiple space objects are involved. As a result, this type of processing loses much of the advantage of general perturbations techniques, namely generally faster state propagation. Although TLE's comprise a specific type of mean orbital elements, propagation tools such as Simplified General Perturbations 4 (SGP4) typically generate (as output) a Cartesian state vector (i.e., position and velocity) in earth-centered inertial (ECI) coordinates. A state estimation tool processing observations to generate a TLE would typically generate the covariance of the mean orbital elements of the TLE, which is generally not as useful for SSA purposes as a Cartesian covariance, which can be transformed into a three-dimensional position probability ellipsoid for uses such as computing probability of collision. The Cartesian covariance is more useful and preferred over the mean orbital elements covariance, neither of which are publicly available.

In this paper, we present a method for quickly propagating Cartesian covariance by computing the state transition matrix using a Lambert targeting routine in lieu of numerical integration, enabling fast multi-rev (even multi-day) analyses commensurate with TLE accuracy. We use Battin's Lambert routine [1] because it is universal, robust, and was designed for quick convergence (minimum iterations). Because any practical conjunction analysis generally requires multiple days of orbit and covariance predictions, we have adapted, in part, Loechler's extension to Battin's method to allow for multi-revolution solutions with no increase in computing time [2]. Furthermore, this fast method enables the estimation of state covariance of space objects from historical TLE data.

2. TRADITIONAL COVARIANCE PROPAGATION

A two-body orbit is completely and uniquely defined by six independent initial conditions, or *orbital elements*. The orbital elements can be expressed in several different forms including the six components of the Cartesian position and velocity vectors, $\bar{r}$ and $\bar{v}$. Combined, the six numbers form the orbital state, or state vector, $X = [x, y, z, \dot{x}, \dot{y}, \dot{z}]^T$. Typically, an estimate of the state X is known at some epoch time. It would be useful to also know the uncertainty of the state X, and how that uncertainty changes with time.

The uncertainty of a multi-variate Gaussian distribution is most often represented by a variance-covariance matrix (often referred to as the "covariance matrix" or simply the "covariance"). The covariance matrix consists of the statistical variance of each of the random variables on the diagonal, and the covariances on the off-diagonals [3]. The linear correlation coefficient between two random variables is a function of the variance and covariance of the two variables. Therefore, the covariance matrix represents the statistical properties of the multi-variate Gaussian distribution. If the covariance changes with time, the ability to propagate it forward or backward in time along with the state X is required. In doing so, the uncertainty of the state will be known at any time, and analyses such as conjunction assessment and prediction of the probability of collision can be performed. Propagating the covariance matrix is traditionally done using the state transition matrix (Φ), which is also, generally, a function of time.

Closed-form solutions of the state transition matrix (STM) exist for certain problems, but the usual technique, especially for orbital work, is to numerically integrate the STM over time [3]. In the linearized orbit prediction problem, the state transition matrix $\Phi(t_2, t_1)$ maps small deviations in the state at time t_1 to some other time t_2.

$$\begin{bmatrix} \delta\bar{r}_2 \\ \delta\bar{v}_2 \end{bmatrix} = \Phi(t_2, t_1) \begin{bmatrix} \delta\bar{r}_1 \\ \delta\bar{v}_1 \end{bmatrix} \tag{1}$$

The STM is computed by numerically integrating the differential equations

$$\dot{\Phi} = F\Phi = \begin{bmatrix} [0_{3\times3}] & [I_{3\times3}] \\ [G(\bar{r}(t))] & [0_{3\times3}] \end{bmatrix}_{6\times6} \Phi \tag{2}$$

with the initial conditions

$$\Phi(t_1, t_1) = [I_{6\times6}] \tag{3}$$

The matrix $[G(\bar{r}(t))]$ is the 3×3 gravity gradient matrix. It is a function of the state, which is integrated simultaneously with the STM. The two-body gravity gradient matrix is [1]

$$[G(\bar{r}(t))] = \frac{\mu}{r^5} \begin{bmatrix} 3x^2 - r^2 & 3xy & 3xz \\ 3yx & 3y^2 - r^2 & 3yz \\ 3zx & 3zy & 3z^2 - r^2 \end{bmatrix} \tag{4}$$

Other useful properties of the STM are

$$\begin{aligned}\Phi(t_1, t_2) &= \Phi^{-1}(t_2, t_1)\\ \Phi(t_3, t_1) &= \Phi(t_3, t_2)\Phi(t_2, t_1)\end{aligned} \tag{5}$$

After the STM has been numerically integrated from t_1 to t_2, the covariance matrix P_1 can also be mapped over time using [3]

$$P_2 = \Phi(t_2, t_1)P_1\Phi^T(t_2, t_1) \tag{6}$$

The numerical integration of the state and the STM is actually the simultaneous integration of forty-two differential equations – six for the state and thirty-six for the STM. This process requires a relatively large amount of computing time, even modeling simple two-body motion. It requires even more computing time to model perturbations, especially when dealing with multiple space objects and long periods of time (i.e. days).

3. LAMBERT STATE TRANSITION MATRIX

The *Lambert problem* is the determination of the two-body trajectory that traverses two specific points in a specific time of flight. It is a fundamental boundary value problem of astrodynamics. Because the Lambert problem operates on the boundary conditions of the trajectory (i.e., the position and velocity vectors at time t_1 and time t_2), the known positions ($\bar{r}_1$ and $\bar{r}_2$) can be systematically varied and the Lambert routine can be used to determine the effects on the velocity at both boundaries. This is essentially the same information conveyed by the STM. The STM can therefore be approximated using Lambert routines. The derivation shown below for approximating the STM using Lambert routines is from [2], which also includes a complete algorithm in pseudocode form.

The STM can be partitioned into sub-matrices as

$$\Phi(t_2, t_1) = \begin{bmatrix} \dfrac{\partial \bar{r}_2}{\partial \bar{r}_1} & \dfrac{\partial \bar{r}_2}{\partial \bar{v}_1} \\ \dfrac{\partial \bar{v}_2}{\partial \bar{r}_1} & \dfrac{\partial \bar{v}_2}{\partial \bar{v}_1} \end{bmatrix}_{6\times 6} = \begin{bmatrix} \Phi_1 & \Phi_2 \\ \Phi_3 & \Phi_4 \end{bmatrix} \tag{7}$$

The STM can be approximated quite well, without any numerical integration, by systematically perturbing the boundary conditions from the nominal and using the Lambert algorithm to determine the effects. The Lambert algorithm is invoked six times, but much less computing time is required, in general, compared to numerical integration of eq. (2). Consider the first row of terms extracted from eqs. (1) and (7).

$$\delta\bar{r}_2 = \frac{\partial \bar{r}_2}{\partial \bar{r}_1}\delta\bar{r}_1 + \frac{\partial \bar{r}_2}{\partial \bar{v}_1}\delta\bar{v}_1 = \Phi_1\delta\bar{r}_1 + \Phi_2\delta\bar{v}_1 \tag{8}$$

Each component of the target point $\bar{r}_2$ can be perturbed in-turn by a small amount δr, while leaving $\bar{r}_1$ unperturbed ($\delta\bar{r}_1 = \bar{0}$). The Lambert algorithm is then run using $\bar{r}_1$ and the perturbed $\bar{r}_2$ to compute the resulting velocity change $\delta\bar{v}_1 = \bar{v}_{1p} - \bar{v}_1$, where $\bar{v}_{1p}$ is the perturbed initial velocity and $\bar{v}_1$ is the nominal. The process is repeated three times, once for each component of $\bar{r}_2$, and the 3x3 matrix $[\delta\bar{v}_1]$ is formed column-by-column from the resulting three $\delta\bar{v}_1$ vectors.

$$[\delta\bar{v}_1]_{3\times 3} = \left[\begin{array}{c|c|c} \delta\dot{x}_1^a & \delta\dot{x}_1^b & \delta\dot{x}_1^c \\ \delta\dot{y}_1^a & \delta\dot{y}_1^b & \delta\dot{y}_1^c \\ \delta\dot{z}_1^a & \delta\dot{z}_1^b & \delta\dot{z}_1^c \end{array}\right] \tag{9}$$

Here the superscripts a, b, c are associated with the three runs of the Lambert algorithm. Likewise, the three $\delta\bar{r}_2$ vectors form the columns of matrix $[\delta\bar{r}_2] = \delta r[I_{3x3}]$. Equation (8) is then solved for Φ_2, recalling that $\delta\bar{r}_1 = \bar{0}$ in all three cases.

$$\Phi_2 = \frac{\partial \bar{r}_2}{\partial \bar{v}_1} \approx [\delta\bar{r}_2][\delta\bar{v}_1]^{-1} = \delta r[I_{3\times 3}][\delta\bar{v}_1]^{-1} = \delta r[\delta\bar{v}_1]^{-1} \tag{10}$$

In a similar manner, Φ_4 is computed from the second row of terms extracted from eqs. (1) and (7)

$$\delta\bar{v}_2 = \frac{\partial \bar{v}_2}{\partial \bar{r}_1}\delta\bar{r}_1 + \frac{\partial \bar{v}_2}{\partial \bar{v}_1}\delta\bar{v}_1 = \Phi_3\delta\bar{r}_1 + \Phi_4\delta\bar{v}_1 \tag{11}$$

$$\Phi_4 = \frac{\partial \bar{v}_2}{\partial \bar{v}_1} \approx [\delta \bar{v}_2][\delta \bar{v}_1]^{-1} \tag{12}$$

where $[\delta \bar{v}_2]$ is the 3x3 matrix with columns comprised of the three difference vectors $\delta \bar{v}_2 = \bar{v}_{2p} - \bar{v}_2$, similar to eq. (9). Note that the matrix inverse needs to be computed only once – the matrix $[\delta \bar{v}_1]^{-1}$ is the same in eqs. (10) and (12).

Partition Φ_3 can be computed from eq. (11) by perturbing the components of $\bar{r}_1$ in-turn and running the Lambert algorithm an additional three times, leaving $\bar{r}_2$ unperturbed in each case ($\delta \bar{r}_2 = \bar{0}$).

$$\Phi_3 = \frac{\partial \bar{v}_2}{\partial \bar{r}_1} \approx \frac{([\delta \bar{v}_2] - \Phi_4[\delta \bar{v}_1])}{\delta r} \tag{13}$$

Partition Φ_1 can be solved from eq. (8) using the results of the same three Lambert algorithm runs.

$$\Phi_1 = \frac{\partial \bar{r}_2}{\partial \bar{r}_1} \approx -\frac{\Phi_2[\delta \bar{v}_1]}{\delta r} \tag{14}$$

Note that no matrix inversion is required. Alternatively, Φ_1 can be derived from the property of the STM that requires the partitions to be interdependent, as in Battin[1] eq. (9.54).

$$\Phi_1 = \left[\Phi_4^{-1}\left([I_{3\times 3}] + \Phi_3 \Phi_2^T\right)\right]^T \tag{15}$$

This equation is slightly more complex than (14), but it forms a more cohesive STM by ensuring the four partitions are truly interdependent. The interdependent partition property holds for two-body and higher order gravity due to the symmetry of the gravity gradient matrix.

3.1. Multi-Rev Lambert Problem

When the Lambert problem time of flight is greater than one orbital period, there are two possible solutions – a high energy and a low energy trajectory. To use the Lambert STM with TLE's over multiple orbits, the "correct" trajectory corresponding to the TLE must be determined. It is critical to determine the total number of full orbits ("revs") N and to determine if the trajectory is the high or low energy solution.

The SGP4 propagator is first run to determine the initial state $\bar{r}_1$ and $\bar{v}_1^*$ at time t_1, and final state $\bar{r}_2$ and $\bar{v}_2$ at time t_2. The semimajor axis and the period of the orbit are then computed.

$$a = \left(\frac{2}{r_1} - \frac{v_1^{*2}}{\mu}\right)^{-1} \tag{16}$$

$$P = 2\pi\sqrt{\frac{a^3}{\mu}} \tag{17}$$

The integer number of full revs is then

$$N = \text{floor}\left(\frac{\Delta t}{P}\right) \tag{18}$$

where the *floor* function returns the integer part of the argument. If $N > 0$ the Lambert algorithm is run to compute both the high and low energy solutions. The specific mechanical energy of each solution is compared to that of the solution generated from the TLE by the SGP4 propagator.

$$E = \frac{v^2}{2} - \frac{\mu}{r} = -\frac{\mu}{2a} \tag{19}$$

The Lambert solution trajectory with energy nearest to that of the TLE trajectory is selected as the final solution, and the Lambert STM routine is then run to compute the associated STM.

4. ESTIMATING TLE COVARIANCE

Although TLE covariance is not publicly available, a covariance matrix can be estimated by various means such as those shown in [4] and [5]. We developed an alternate method of estimating covariance based on historical TLE data. For an entire set of TLEs, each TLE is propagated forward in time to the epoch time of the final TLE in the set. Transform all of the position and velocity vectors at the final epoch from ECI coordinates to the radial, in-track, cross-track (RIC) coordinate system of the final TLE. The RIC unit vectors are computed using

$$\hat{R} = \bar{r}/r, \quad \hat{C} = (\bar{r} \times \bar{v})/|\bar{r} \times \bar{v}|, \quad \hat{I} = \hat{C} \times \hat{R} \tag{20}$$

The ECI to RIC transformation matrix is then formed by making these unit vectors the *rows* of the matrix.

$$T_{RIC|ECI} = \begin{bmatrix} \hat{R}^T \\ \hat{I}^T \\ \hat{C}^T \end{bmatrix}_{3\times 3} \tag{21}$$

The transformed position and velocity vectors at the final epoch indicate the measure of uncertainty of the set of TLEs over the time span from the first TLE to the last. An RIC covariance matrix can be computed from the final position and velocity data. This covariance matrix can be transformed to the ECI system and mapped back to time t_1 using the inverse of the Lambert STM. The covariance is then transformed into the RIC system of the first TLE in the set. Doing so essentially makes the covariance independent of the ECI conditions of the TLE. It can then be used as the representative covariance for TLEs of that particular space object at any TLE epoch.

5. TEST AND VALIDATION

To test and validate the Lambert STM method for quickly propagating TLE covariance, two example orbiting objects were used – the LAGEOS satellite and the International Space Station (ISS). An example 4σ position probability ellipsoid for LAGEOS is shown in Fig. 1. The ellipsoid (in black) was derived from the covariance matrix computed

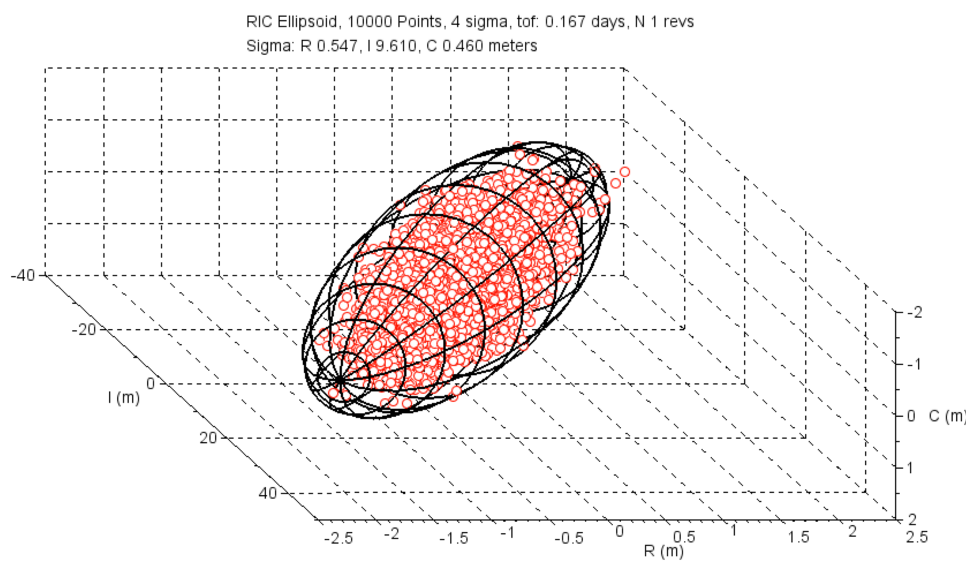

Fig. 1: LAGEOS example 3D. 4σ probability ellipsoid, position, in RIC.

by the Lambert STM on an actual LAGEOS TLE. The propagation time was four hours, somewhat greater than one LAGEOS orbit period. A set of $10,000$ random test points (Gaussian distribution) were generated about the epoch position and velocity of the TLE and propagated forward using universal variable methods [6]. The final states of the test points were transformed to the RIC frame at the final epoch and were plotted (in red) in Fig. 1. The figure shows that the covariance matrix computed by the fast Lambert STM method represents very well the estimated position uncertainty properties of the propagated TLE, including the correlation between the radial and in-track components.

5.1. LAGEOS Tests

A set of nine TLEs covering approximately five days was used to estimate the covariance of the LAGEOS TLEs. The 4σ probability ellipsoid at the final epoch is shown in Fig. 2. This is a non-isometric figure – note the large scale

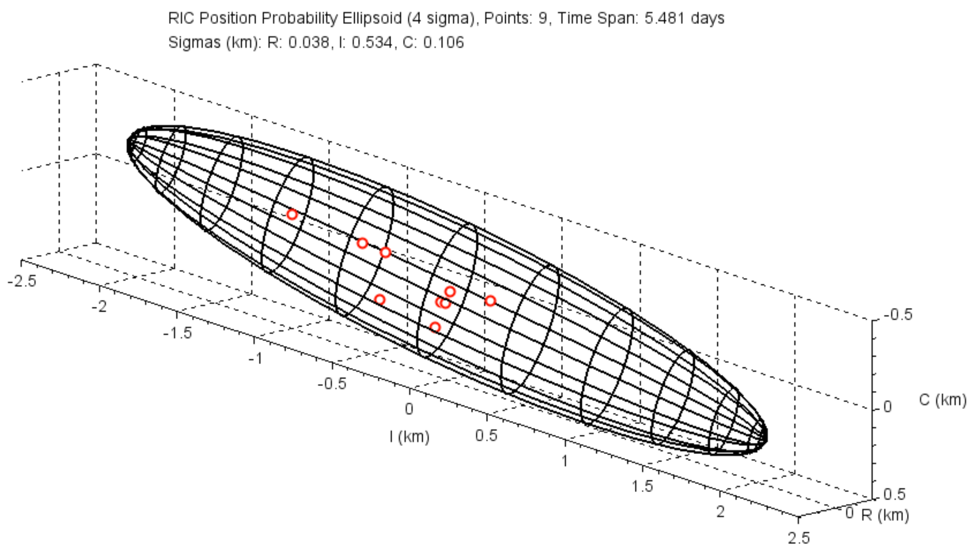

Fig. 2: LAGEOS estimated covariance (4 σ) from propagated TLEs.

differences between the three axes. As expected, most of the dispersion is in the in-track direction. The associated ECI covariance matrix was mapped back in time to the epoch of the first TLE in the set. A set of 1,000 Gaussian random points were propagated forward from the initial TLE epoch using the associated Lambert STM, and the resulting covariance was computed from the propagated random points. The final points and the associated RIC position probability ellipse of the radial and in-track components are shown (in red) in Fig. 3. Also shown in the figure (in black) for comparison are the random points propagated by universal variables and the associated probability ellipse. The figure shows that the Lambert STM method captures the uncertainty properties very well.

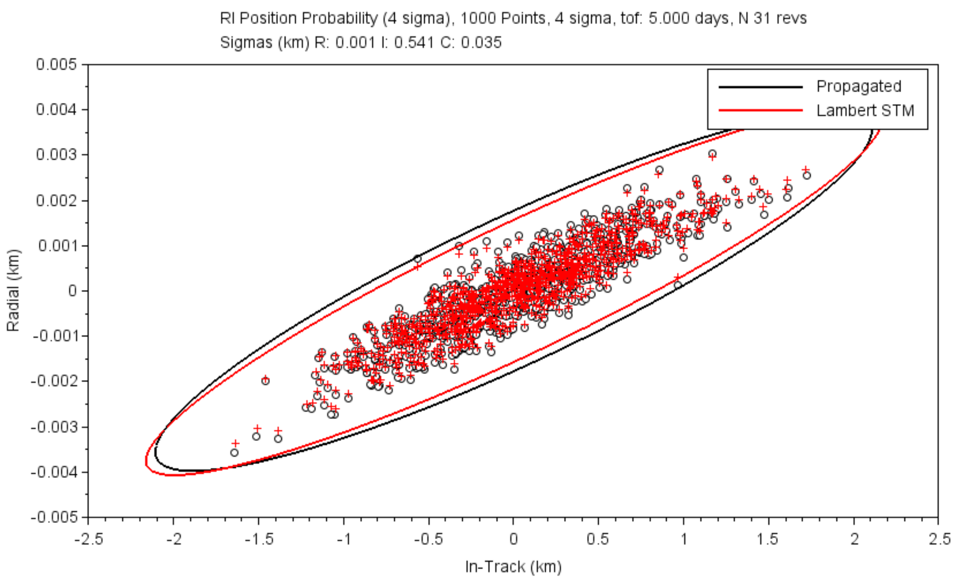

Fig. 3: LAGEOS RI ellipses.

5.2. International Space Station (ISS) Tests

A similar test was conducted using TLEs of the International Space Station (ISS). The ISS is in a lower, faster moving orbit and is much larger in size compared to LAGEOS (i.e., greater drag). As before, a set of 20 TLEs over a 3 day period (approximately) was used to estimate the covariance of the ISS TLEs. The resulting RIC position ellipsoid is shown in Fig. 4. As expected, there is much more dispersion in the in-track direction compared to the LAGEOS ellipsoid (Fig. 2), even though the time span is shorter, due to the greater speed and drag of the ISS.

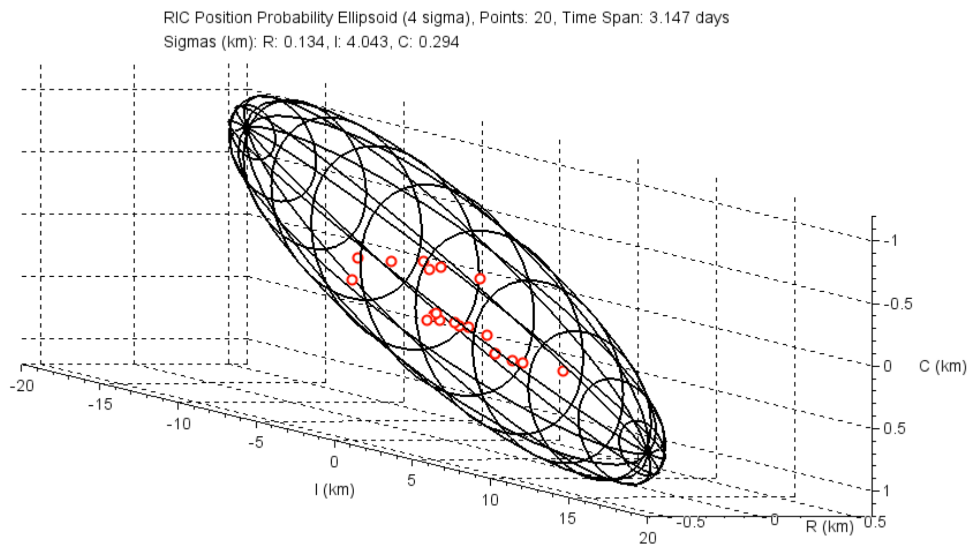

Fig. 4: ISS estimated covariance (4 σ) from propagated TLEs.

The estimated covariance was mapped back to the initial TLE epoch. A set of 1,000 random test points were propagated using the Lambert STM and universal variables, and the uncertainty properties of the final distributions were computed. The associated probability ellipsoids are shown in Fig. 5. Again we see a very good match between the two sets of random test points. Note the very large difference in scale between the two axes of the plot. This tends to visually amplify errors in the radial direction (vertical axis).

Some non-Gaussian properties of the universal variable random points can be seen in Fig. 5. This becomes even more apparent when a longer time span is used. Figure 6 shows the random points distribution of a seven-day propagation time span. It is interesting to note that the Lambert STM method apparently preserves the Gaussian nature of the random points. However, the true nature of the uncertainty propagated over time may not remain Gaussian. This is an area of potential investigation in future research.

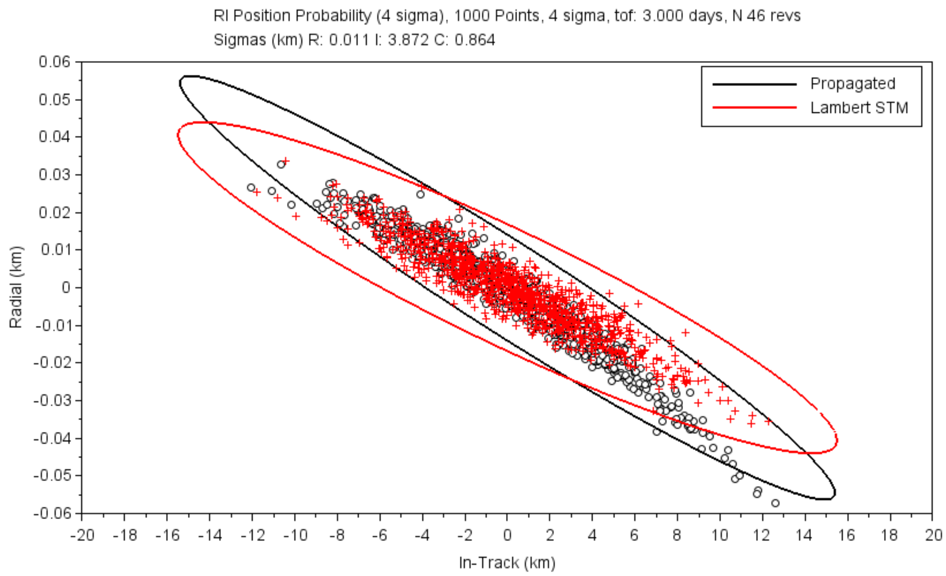

Fig. 5: ISS RI ellipses.

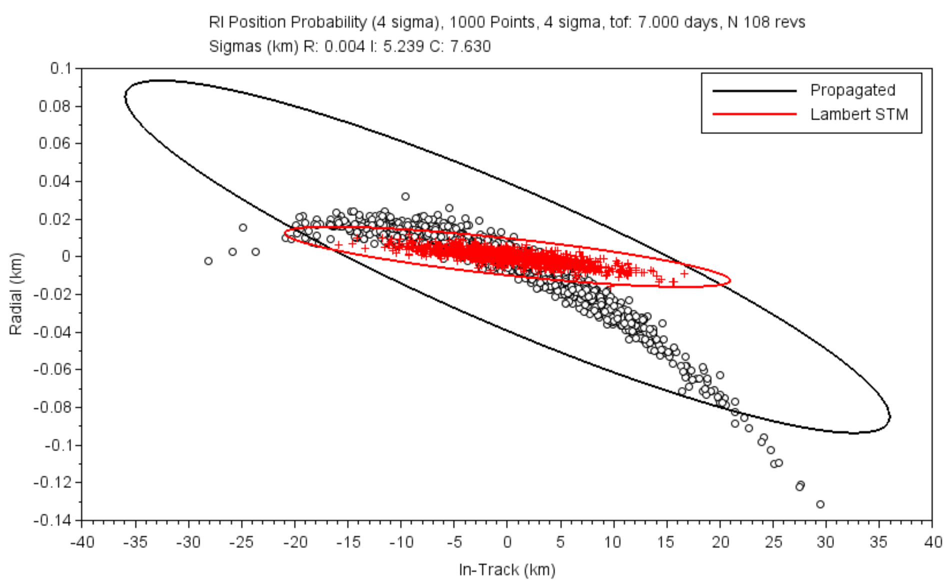

Fig. 6: ISS RI ellipses, 7 days time span.

6. SUMMARY

Two-line element set (TLEs) are publicly available and widely used to track thousands of orbiting objects. They generate medium accuracy trajectories using general perturbation methods. However, no covariance or other measure of uncertainty is published with the TLEs, making them less useful for certain space situational awareness (SSA) purposes such as conjunction prediction and analysis. The Cartesian covariance of a TLE can be estimated by various methods, but propagating the covariance by traditional numerical methods can consume unreasonable computing time and resources. This is especially true for long propagation periods (i.e., days) and multiple space objects. We present a method for using Lambert targeting routines to very quickly approximate the state transition matrix used to propagate the covariance matrix. The length of the propagation time has no effect on the speed at which the new method operates. Additionally, we present a novel method for estimating the covariance from a historical set of TLEs. These methods can be used to enable SSA analysis methods at time spans currently not practical using TLEs.

7. DISCLAIMER

The views expressed in this paper are those of the authors and do not reflect the official policy or position of the United States Air Force, Department of Defense, or the U.S. Government.

References

[1] Battin, R. H., *An Introduction to the Mathematics and Methods of Astrodynamics*, AIAA Education Series, American Institute of Aeronautics and Astronautics, Inc., New York, 1987.

[2] Thompson, B., D. Brown, R. Cobb, “Complete Solution to the Lambert Problem with Perturbations and Target State Sensitivity,” AAS 18-074, *Advances in the Astronautical Sciences*, Vol. 164, 2018, pp.421-432.

[3] Tapley, B., Schutz, B., Born, G., *Statistical Orbit Determination*, Elsevier Academic Press, Amsterdam, 2004.

[4] Osweiler, V., *Covariance Estimation and Autocorrelation of NORAD Two-Line Element Sets*, M.S. thesis, Air Force Institute of Technology, Mar 2006.

[5] Yurong, H., L. Zhi, H. Lei, *Covariance Propagation of Two-Line Element Data*, 2016 Chinese Control and Decision Conference (CCDC), listed in IEEE Xplore digital library, 2016. doi: 10.1109/CCDC.2016.7531654

[6] Vallado, D., *Fundamentals of Astrodynamics and Applications*, 4th ed., Microcosm Press, Hawthorne, California, 2013.

[7] Hoots, F., R. Roehrich, *Models for Propagation of NORAD Element Sets*, Spacetrack Report #3, Aerospace Defense Command, U.S. Air Force, 1980.

[8] Vallado, D., P. Crawford, R. Hujsak, T.S. Kelso, *Revisiting Spacetrack Report #3*, rev 2, AIAA 2006-6753-Rev2, 2006.

[9] Vallado, D., P. Cefola, *Two-Line Element Sets - Practice and Use*, IAC-12-A6.6.11, 63rd International Astronautical Congress, Naples, Italy, 2012.

[10] Space-Track.org, Joint Functional Component Command for Space (JFCC SPACE), US Air Force, https://www.space-track.org

[11] Thompson, B., “Enhancing Lambert Targeting Methods to Accommodate 180-Degree Transfers,” *Journal of Guidance, Control, and Dynamics*, Vol. 34, No. 6, 2011, pp.1925-1929.